ACS OMEGA

http://pubs.acs.org/journal/acsodf

Article

9-Trifluoromethylxanthenediols: Synthesis and Supramolecular Motifs

Manuel Rodríguez-Molina,* Dazaet Galicia-Badillo, Enoc Cetina-Mancilla, Jorge Cárdenas, Lilian I. Olvera, Rubén A. Toscano, Braulio Rodríguez-Molina,* and Mikhail G. Zolotukhin

Cite This: *ACS Omega* 2022, 7, 13520−13528

Read Online

ACCESS | Metrics & More | Article Recommendations | Supporting Information

ABSTRACT: The synthesis of four derivatives and the single-crystal X-ray structures of six 9-trifluoromethylxanthenediols (TFXdiols) **I**−**VI** are analyzed in this work. These compounds were obtained through superacid-catalyzed condensation of dihydroxybenzenes with 1,1,1-trifluoroacetone or 2,2,2-trifluoroacetophenone. The title molecules have a convex molecular structure due to their three fused rings of the xanthene moiety. We have found that, similar to resorcinol, the configuration of the hydroxyl groups is of great relevance for the crystal packing favoring either interactions above and below their molecular plane or lateral interactions that create layers. Considering that reports of TFXdiols are very scarce, our findings contribute to a better understanding of the molecular conformation and intermolecular interactions in their crystal structures. A similar analysis was extended to a fortuitous cocrystal obtained between 9-trifluoromethyl-9-(4′-fluorophenyl)-xanthenediol and 1,4-dihydroxybenzene, showing that these structures might be used to obtain cocrystals in the future.

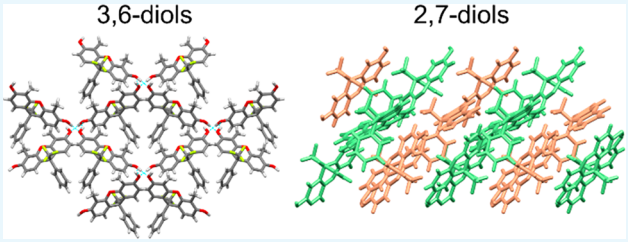

INTRODUCTION

Xanthene-containing molecules have been widely studied due to their numerous applications that take advantage of their biological and pharmacological properties.[1−7] They have also attracted interest due to their interesting photophysical properties, as some derivatives can be used as pigments, dyes, and biological sensors.[8−14] In addition, xanthene fragments have been used as an essential constituent in polymers chains.[15−20] Xanthene fragments are critical components for constructing polymer layered p-electron systems,[16−18] as well as polymers for gas separations or sorption, and membranes.[19,21,22] Among those, fluorine-containing xanthenes can be used to prepare high-performance heteroaromatic polymers, such as polyimides,[23] polyarylethers, and polybenzoxazoles.[24] Particularly, the introduction of $-CF_3$ groups in the structure has been one of the most widely used strategies to obtain solution-processable polymers, a highly desired property that enables attractive applications.[25,26]

Some of us have reported the preparation of soluble polymers based on the condensation of biphenol and 2,2,2-trifluoroacetophenone in superacid conditions.[27] In addition, we also employed the symmetric xanthenediol 3,6-dihydroxy-9-trifluoromethyl-9-phenylxanthene (**III**) to obtain a highly soluble and fully aromatic ladder polymer with excellent gas permselectivity performance.[28] By extending the developed approach, new polymers could be obtained using other xanthenediol derivatives.

The xanthene moiety is frequently encountered in the literature (Figure 1a). A recent search in the Cambridge

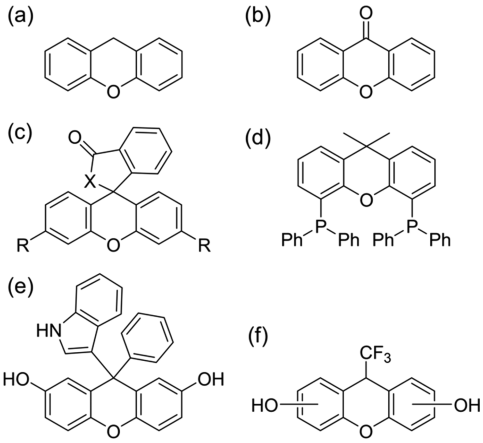

Figure 1. (a) Xanthene motif (2357 entries in the CCDC). (b) 9-Xanthone motif (264 entries in the CCDC). (c) Xanthene dye skeleton motif (X = O, N, R = −OH, $-N(Et)_2$, 411 entries in the CCDC). (d) Xantphos ligand (423 entries in the CCDC). (e) Related xanthenediol derivative (CCDC code: HORMUZ). (f) 9-Trifluoromethyxanthenediol (TFXdiol) skeleton (1 entry in the CCDC).

Received: November 23, 2021
Accepted: March 31, 2022
Published: April 13, 2022

https://doi.org/10.1021/acsomega.1c06635
ACS Omega 2022, 7, 13520−13528

Crystallographic Data Centre,[29] performed using ConQuest 2021.1.0 software,[30] indicates that approximately 2350 related structures have been deposited, including 9-xanthones (Figure 1b), xanthene dyes (Figure 1c), or xantphos-related structures (Figure 1d). A xanthenediol structure can also be found in the recent work from Niu and collaborators (HORMUZ, Figure 1e).[31] Nevertheless, to this date, only one TFXdiol structure has been reported in detail so far (Figure 1f). The reported 3,6-dimethyl-9-phenyl-9-trifluoromethyl-9*H*-xanthene-2,7-diol was used as an intermediate in the obtaining quinone-hydroquinone hybrid structures in stereodynamic redox reactions.[32] Furthermore, only a handful of studies focused on the structure of xanthenes derivatives have been reported, for example, the 9-substituted-9-xanthenol clathrates studied by Taljaard and co-workers,[33,34] the 1,8-dioxooctahydroxanthenes analyzed by da Silva and collaborators,[35] the 9-substituted-9-phenylxanthenes reported by Kavala and others,[36] or mechanochemical cocrystallization of fluorescein by Bučar and others.[37]

Considering the above, in this work, we report the synthesis and structural analysis of four 9-trifluoromethyldihydroxyxanthenediols (TFXdiols). The title compounds were synthesized through condensation catalyzed by trifluoromethanesulfonic acid (TFSA) between resorcinol or hydroquinone and trifluoromethyl ketones.[38] Gratifyingly, the resulting compounds show a high tendency to crystallize. It is considered that the study of these X-ray structures would help to establish the most common solid-state conformations and to determine the governing intermolecular interactions (Figure 2a). To facilitate the description of TFXdiols structures, in this work a common numbering system was used for all structures (Figure 2b, Figure S13).

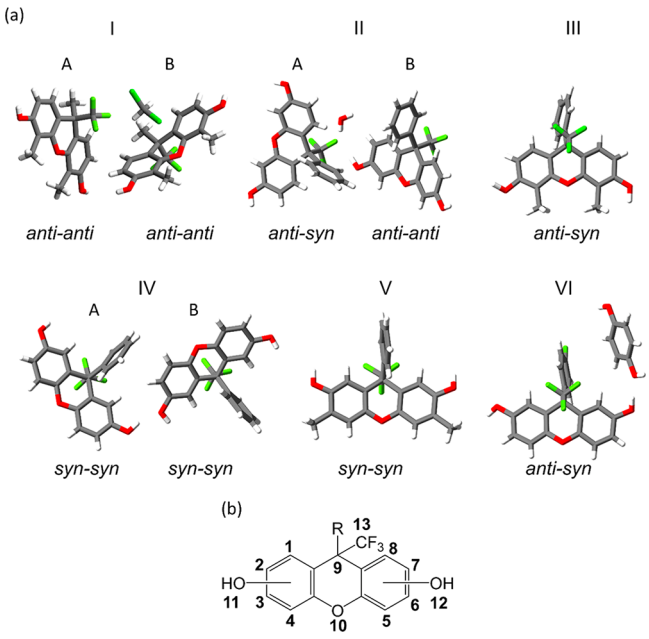

Figure 2. (a) Molecules and diol conformations in the asymmetric units of compounds **I**–**VI**. When two molecules per asymmetric unit are found, labels A and B are employed. Compounds **III** and **V** have been published before and were included here only to provide a broader perspective of the packing motifs. (b) Numbering system of this work employed to consistently describe the observed intermolecular interactions.

RESULTS AND DISCUSSION

Synthesis and Characterization of Compounds 1–5. Compounds **1**–**5** were obtained through the reaction of 1,1,1-trifluoroacetone or 2,2,2-trifluoroacetophenone with the appropriate dihydroxybenzene derivative (either hydroquinone, resorcinol, or 2-methylresorcinol) and TFSA in dichloromethane (DCM) at 10 °C (Scheme 1, left). Good yields of each molecule were obtained, and their complete characterization was carried out with diverse analytical techniques as ^{1}H, ^{13}C, and ^{19}F NMR, IR spectroscopy, and mass spectrometry (see Supporting Information). Single crystals suitable for X-ray diffraction were obtained through slow evaporation of saturated solutions of the compounds in DCM. The most relevant crystallographic parameters are compiled in Table 1.

Molecular Structures of I–VI by Single-Crystal X-ray Diffraction Studies. This section presents relevant intermolecular interactions of the compounds **I**–**VI** and some conformation similarities with other diols. Although there are no systematic studies of other three-ring-fused diols (for example, anthracene, acridine, phenazine, or xanthene), it is possible compare them with the simplest aromatic planar diol, resorcinol. Resorcinol can show polymorphism associated with its conformers. The polymorph α consists of molecules where the diols adopt an anti−anti conformation, while in polymorph β the hydroxyl groups adopt a syn−anti conformation.[39] Additionally, a syn−syn conformer is frequently encountered in crystal engineering or cocrystals.[40] Furthermore, the three possible conformations can be founded in the orcinol form II polymorph.[41] Interestingly, despite their size, the TFXdiols structures can be considered as an extended series of orcinol because these conformations were found in their X-ray structures.

The xanthene molecules depart from planarity due to the sp^3 oxygen atom that lies on the center of the fused rings. The concave shape can be described by θ, which is the angle created by the intersecting planes of the aromatic rings (Figure 3a). Table 2 contains the θ values found in each compound reported here. The angles θ range from 154.4° in **I** (the more concave structure) to 169.8° in **IV** (the more planar structure). In crystal **I**, each of the two molecules of the asymmetric unit has its own θ angle, with a difference of 12°.

Similarly, the torsion of the phenyl ring at C9 in structures **II**–**VI** can be described by φ, which indicates the angle between the relative position of this substituent and the closest aromatic ring in the xanthene framework. The values of φ range from 79.26° in **III** to 69.2° in **IV**. In the structure **IV** which contains two molecules in the asymmetric unit, φ differs by 10° in each molecule (Table 2).

To evaluate the similarity between all the molecular conformations and their molecular packings, we performed an in-depth analysis using CrystalCMP.[42] This visualizing tool allowed us to confirm that the conformation is comparable across all compounds, despite the variations the θ and φ angles, as illustrated in the overlay of Figure 3b, with the root-mean-square values included in Figure S14.

Molecular Packing of TFXdiols I–III. After the conformational differences in the crystal structures were established, the intermolecular interactions of the TFXdiols will be described in this section. We start from structure **I**, and subsequently we will present the 3,6-xanthenediols **II** and **III**. The latter molecules differ from **I** because they feature a phenyl ring

https://doi.org/10.1021/acsomega.1c06635
ACS Omega 2022, 7, 13520−13528

Scheme 1. Left: Synthesis of 9-Trifluoromethylxanthenediols (TFXdiols). Right: Chemical Structures I–VI Analyzed in This Work[a]

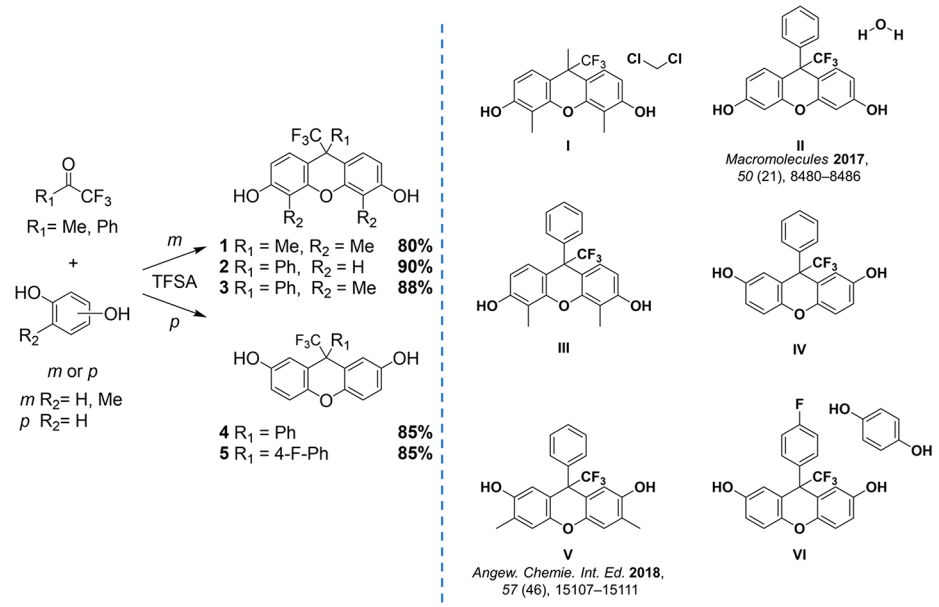

[a]The structures of compounds **II** and **V** have been reported before[28,32] and are included here for a better description of TFXdiols structures.

Table 1. Selected Crystallographic Data of Crystals I, II, IV, and VI (CCDC Deposit Number)

	I (2122963)	**III** (2122965)	**IV** (2122966)	**VI** (2122964)
formula	$3(C_{17}H_{15}F_3O3)$, CH_2Cl_2	$C_{22}H_{16}F_3O_3$	$C_{20}H_{13}F_3O_3$	$C_{23}H_{15}F_4O_4$
MW/g mol^{-1}	1057.79	385.35	358.30	431.35
T/K	298	298	150	298
crystal system	orthorhombic	orthorhombic	monoclinic	monoclinic
space group	*Pnma*	$Pna2_1$	$P2_1/c$	$P2_1/c$
a/Å	20.3374(5)	7.7794(3)	9.3314 (10)	13.227(4)
b/Å	28.1705(7)	19.3621(7)	25.917 (3)	6.4241(17)
c/Å	8.7934(2)	12.6018(4)	13.5289 (15)	22.762(6)
α (deg)	90	90	90	90
β (deg)	90	90	106.616 (4)	97.892(11)
γ (deg)	90	90	90	90
V/Å^3	5037.9(2)	18998.1(2)	3135.2 (6)	1915.9(9)
Z	4	4	8	4
Z'	1.5	1	2	1
ρ/g cm^{-3}	1.395	1.348	1.518	1.495
μ/mm^{-1}	1.938	0.926	1.075	0.127
F(000)	2184	796	1472.0	884
radiation/Å	CuKα 1.54178	CuKα 1.54178	CuKα 1.54178	MoKα 0.71073
reflections collected	35112	30831	88177	42888
independent reflections	5513 [R(int) = 0.1047]	3865 [R(int) = 0.0580]	6648 [R(int) = 0.0592]	5570 [R(int) = 0.0413]
data/restraints/parameters	5513/3/350	3865/1141/515	6648/0/481	5570/3/289
goodness of fit on F^2	1.036	1.051	1.044	1.045
final R indices [$I > \sigma(I)$]	R_1 = 0.0661, wR_2 = 0.1653	R_1 = 0.0458, wR_2 = 0.1115	R_1 = 0.0362, wR_2 = 0.0918	R_1 = 0.0531, wR_2 = 0.1136
R indices (all data)	R_1 = 0.1139, wR_2 = 0.1978	R_1 = 0.0684, wR_2 = 0.1384	R_1 = 0.0413, wR_2 = 0.0958	R_1 = 0.0874, wR_2 = 0.1288

adjacent to the $-CF_3$ moiety. It is important to note that structure **II** was previously reported by some of us,[28] but it was included here because its molecular packing was not described in detail before.

The crystal of **I** was solved in the orthorhombic system, *Pnma* space group. It contains one and a half molecules of xanthenediol and a molecule of dichloromethane (DCM) per asymmetric unit (Figure 4a). Despite being occluded within the crystalline lattice, the DCM molecules do not establish strong intermolecular interactions with the xanthenediol derivative. Conversely, the hydroxyl groups in the TFXdiol adopt an anti–anti conformation and established three $C_1^1(3)$ O–H···O hydrogen bonds with oxygen–oxygen distances d = 2.700(3), 2.792(3), and 2.773(3) Å and angles of 171(5)°, 169(5)°, and 163(5)° respectively for the motif. Considering the length and angles of these hydrogen bonds, they can be cataloged as moderate,[43] with chains that extend over the three directions of the unit cell (Figure 4b). The parameters of these

https://doi.org/10.1021/acsomega.1c06635
ACS Omega 2022, 7, 13520–13528

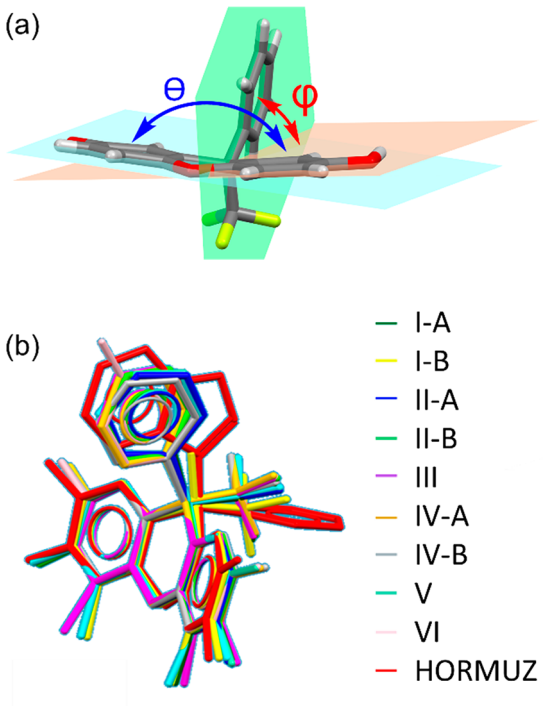

Figure 3. (a) Concave structure of TFXdiols exemplified by structure **IV**. The angle θ and the angle φ are indicated with double-headed arrows; see text for a detailed description. (b) Overlay of the crystallographic independent XTFdiols of the structures in this work. The related xanthenediol structure HORMUZ was included for a better comparison.[31]

Table 2. Compilation of θ and φ Angles in the Structures Discussed Here[a]

structure		θ [deg]	φ [deg]
I	A	166.85	
	B	154.43	
II	A	167.33	78.06
	B	166.14	79.26
III		161.31	69.58
IV	A	169.81	78.34
	B	168.45	69.18
V		166.01	78.48
VI		161.80	75.01

[a]Labels A and B refer to the crystallographically independent molecules.

bonds are compiled in Table 3 to provide a better comparison for all the structures described here.

The structure of crystal **II** was solved in a monoclinic system in the $P2_1/c$ space group with two molecules per asymmetric unit. This disposition gave rise to both anti−syn and anti−anti conformations (Figure 5). Compared to the previous compound, the molecular packing of this concave molecule tends to form two types of head-to-tail pairs (labeled A and B). Pair A is created between molecules that are held together by means of weak $\pi\cdots\pi$ interactions, with a centroid−plane distance of 3.51 Å (Figure 5a).[44] The pair B is held together by two hydrogen bonds (labeled 1 and 2) between −OH groups and adventitious water molecules. The donor−acceptor distances for the hydroxyl−water hydrogen bonds are 2.670(3) and 2.940(3) Å and O−H···O angles of 171(3)° and 155(4)° respectively (Figure 5b, Table 3). Pairs A and B

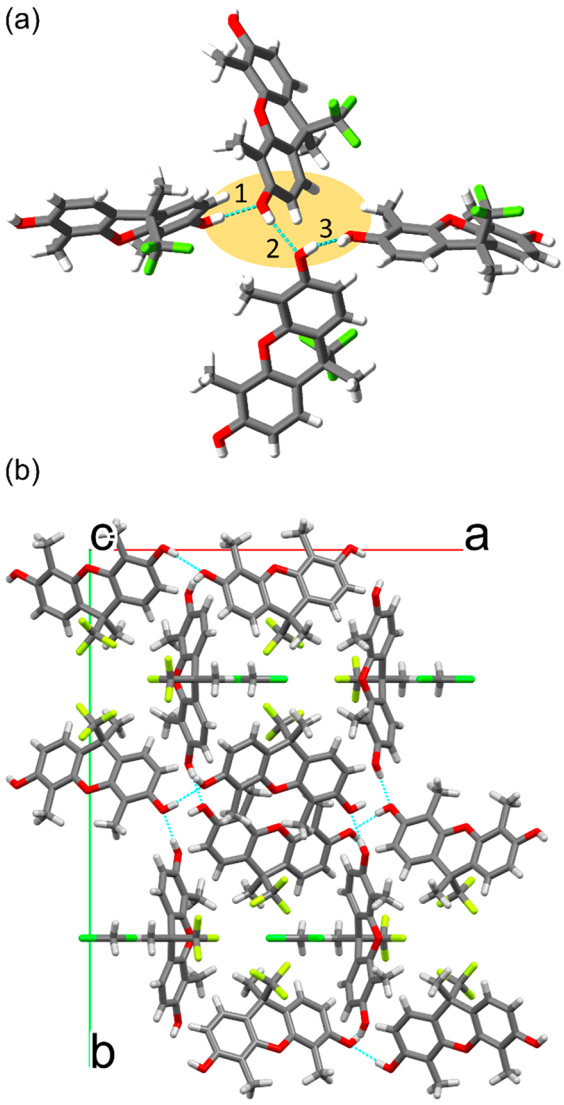

Figure 4. (a) Hydrogen bonds in **I** that propagate the lattice in the three directions. (b) View down the *c*-axis of **I**.

are additionally interconnected through two hydrogen bonds (labeled 3 and 4) between them, with donor−acceptor distances 2.857(2) and 2.776(2) Å, and respective O−H···O angles of 174(4)° and 155(2)°. Finally, a O−H···π bond (labeled 5) with a donor−centroid acceptor distance of 3.56(2) Å and 157(4)° angle was also observed (Figure 5c and Table 3).[45]

Structure **III** belongs to an orthorhombic system, in the space group $Pna2_1$, with one molecule per asymmetric unit (Figure 2). The hydroxyl groups in this structure adopt an anti−syn conformation producing infinite chains with two types of hydrogen bonds $C_1^1(3)$ with donor−acceptor internuclear distances of 2.90(4) and 2.77(2) Å and angles of 151(7)° and 172(8)° respectively (Figure 6a, Table 3). These chains propagate along the three crystallographic axes (Figure 6b).

Interesting differences are observed between **II** and **III**. The hydrogen bonds in **II** only are propagated through the (010) plane, while in **III** they propagate in all three directions. This was attributed to the presence of water molecules in **II** that "block" the interactions in other directions and allow the presence of the two types of −OH conformers.

https://doi.org/10.1021/acsomega.1c06635
ACS Omega 2022, 7, 13520−13528

Table 3. Bond Distances and Angles for the Interactions (O−H···O, O−H···π, C−H···π, and C−H···F) in I−VI

structure	#	H-bond	D−H (Å)	H···A (Å)	D···A (Å)	∠DHA (deg)
I	1	O(12B)−H(12B)···O(12A)	0.78(3)	1.93(3)	2.700(3)	171(5)
	2	O(12A)−H(12A)···O(11A)	0.77(3)	2.03(3)	2.792(3)	169(5)
	3	O(11A)−H(11A)···O(11B)	0.79(3)	2.01(3)	2.773(3)	163(5)
II	1	O(12B)−H(12B)···O(20)	0.88(3)	1.80(3)	2.670(3)	171(3)
	2	O(20)−H(20b)···O(11B)	0.85(2)	2.15(3)	2.940(3)	155(4)
	3	O(20)−H(20a)···O(12A)	0.85(2)	2.01(2)	2.857(2)	174(4)
	4	O(12A)−H(12A)···O(12B)	0.86(3)	1.97(3)	2.776(2)	155(2)
	5	O(11B)−H(11B)···π	0.85(3)	2.76(3)	3.56(2)	157(4)
III	1	O(11)−H(11)···O(12)	0.87(14)	2.14(15)	2.90(4)	151(7)
	2	O(12)−H(12)···O(11)	1.07(11)	1.70(11)	2.77(2)	172(8)
IV	1	O(11B)−H(11B)···O(12A)	0.84(2)	1.98(2)	2.742(2)	151(2)
	2	O(12A)−H(12A)···O(12B)	0.89(2)	1.96(2)	2.814(2)	161(2)
	3	O(12B)−H(12B)···O(11A)	0.85(2)	2.19(2)	2.979(2)	155(2)
	4	O(11A)−H(11A)···O(11B)	0.84(2)	2.00(2)	2.819(2)	164(2)
	5	C(6B)−H(6B)···F(A2)	0.95(2)	2.50(2)	3.34(2)	146(2)
	6	C(6A)−H(6A) ···Cg	0.95(2)	3.34(2)	4.09(2)	137(2)
V	1	O(12)−H(12)···O(11)	0.78(2)	1.93(2)	2.700(2)	171(4)
	2	O(11)−H(11)···π	0.84(2)	2.32(2)	3.050(2)	145(3)
VI	1	O(23)−H(23)···O(12)	0.886(18)	1.88(2)	2.763(2)	175(3)
	2	O(12)−H(12)···O(11)	0.876(17)	1.84(2)	2.706(2)	172(2)
	3	O(11)−H(11)···O(23)	0.879(17)	1.89(2)	2.763(2)	171(2)
	4	C(6)−H(6)···F(13b)	0.93(2)	2.63	3.473	150.6

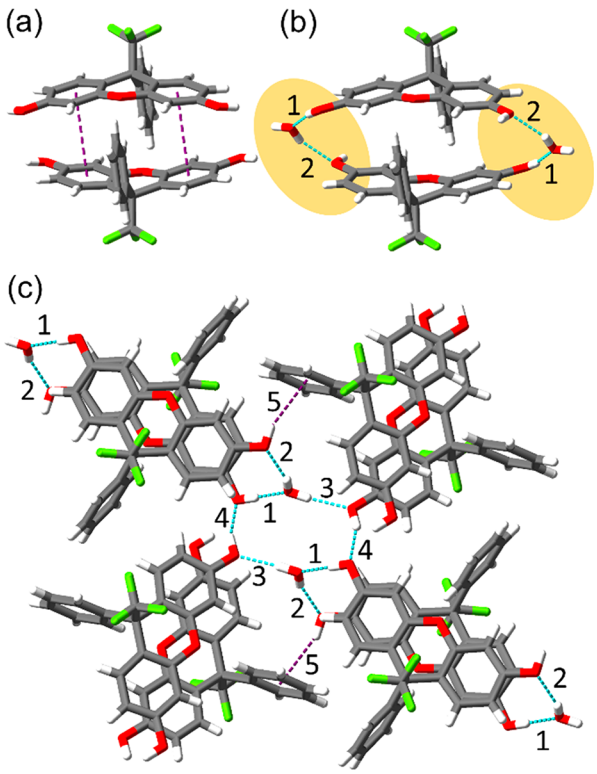

Figure 5. (a) Dimer A formed by π···π interactions in **II**. (b) Dimer B formed by bridging water molecules. (c) Hydrogen bonds between TFXdiol dimers.

Molecular Packing of TFX-Diols IV−VI. After the structures **I−III** were analyzed, interactions of the hydroxyl groups in other positions of the xanthenediol framework can be better compared. Structure **IV** with the hydroxyl groups in positions 2 and 7 was solved in a monoclinic system with a space group $P2_1/c$. It has two molecules per asymmetric unit, and in both the hydroxyl groups adopt a syn−syn

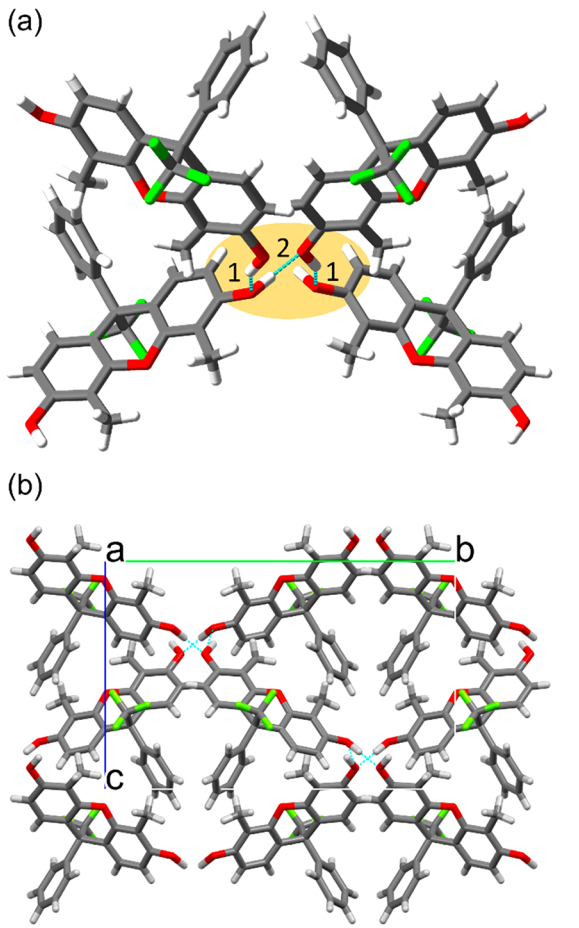

Figure 6. (a) The two types of hydrogen bonds (1 and 2) that propagate the over the three directions in **III**. (b) Crystal packing of **III** viewed through the *a*-axis.

https://doi.org/10.1021/acsomega.1c06635
ACS Omega 2022, 7, 13520−13528

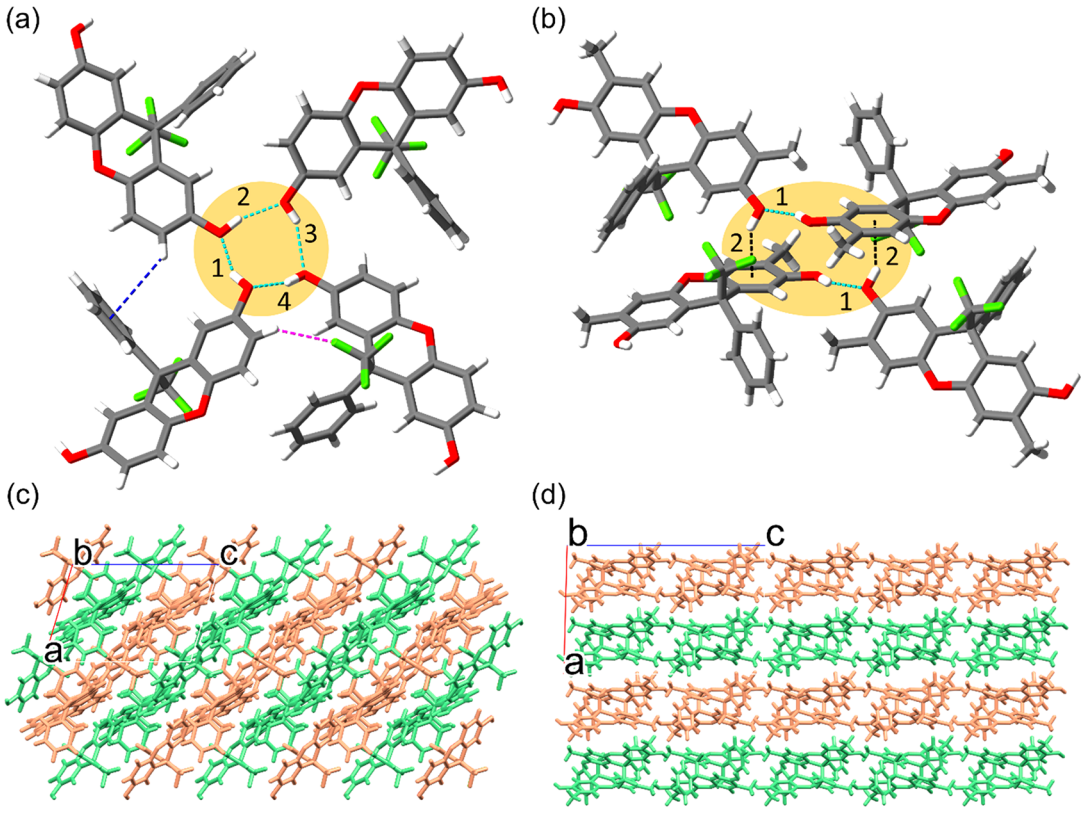

Figure 7. (a) Ring motif, $R_4^4(8)$, of **IV**, as well as CH···π and CH···F interactions. (b) Ring motif of **V** formed by hydroxyl hydrogen bonds. (c) Crystal packing of **IV** viewed through the *b*-axis. Layers in the (101) plane are marked with green and orange colors. (d) Crystal packing of **V** viewed through the *b*-axis. Layers in the (100) plane are marked with green and orange colors.

conformation. In this structure, four types of hydrogen bonds give rise to a $R_4^4(8)$ motif. These hydrogen bonds show donor−acceptor (oxygen−oxygen) distances of 2.742(2), 2.81(2), 2.979(2), 2.819(2) Å and O−H···O angles of 151(2)°, 161(2)°, 155(2)°, and 164(2)° respectively (Table 3). Furthermore, CH···π and CH···F weak interactions were identified, with donor−centroid acceptor distances of 4.09 Å and donor−acceptor distance of 3.34 Å, respectively (Figure 7a, Table 3).

We also include here the previously reported structure **V** to strengthen the comparison of this series.[32] The hydroxyl groups in this molecule adopt a syn−syn conformation, suggesting that the methyl groups may interfere and prevent the motif found in **IV**. Instead, this structure shows an interesting pseudoring formed by two types of hydrogen bonds: two OH···O hydrogen bonds with a donor−acceptor distance of 2.700(2) Å and an angle of 171(4)°, and two OH···π bonds with a donor−centroid acceptor distance of 3.05(2) Å and an angle of 145(4)° (Figure 7b, Table 3). These interactions create layers along the (101) and (100) planes (Figure 7c,d).

Serendipitous Packing of VI. Finally, a brief description of cocrystal **VI** will be provided. This cocrystal was serendipitously obtained during the purification process of compound **5**, and it was included here to suggest that the hydroxyl groups can be used in the future to engineering new cocrystal platforms as have been widely implemented by another diols.[46] This cocrystal was solved in a monoclinic system, in the space group $P2_1/c$, with a xanthene molecule and half of hydroquinone molecule in the asymmetric unit. Unlike structures **IV** and **V**, where the hydroxyl groups adopted syn−syn conformations, the structure **VI** has an anti−syn conformation that could be facilitated by the presence of its hydroquinone coformer. This cocrystal shows a motif in which four xanthene molecules and two hydroquinone molecules interact through three different O−H···O bonds with donor−acceptor distances of 2.763(2), 2.706(2), and 2.762(2) Å and angles of 175(3)°, 172(2)°, and 171(2)° respectively. These bonds give rise to a ring $R_6^6(22)$, with layers in the plane (100). The layers propagate through the *a*-axis by a weak CH···F interaction, with a donor−acceptor distance of 3.473 Å and an angle of 150.6°. Furthermore, additional CF···π weak interactions were observed with a distance between the fluorine atom and the aromatic centroid of 3.241 Å, with an angle of 123.8°.[47]

Divergence of the Arrays of Compounds I−VI. After establishing the high degree of similarity among the conformation of the compounds **I**−**VI**, it was desirable to establish if the molecular packings could show some resemblances. To this end, CrystalCMP was employed again to provide a detailed comparison. The results clearly indicate that all packings are dissimilar (Figure S15), probably due to the presence of water or solvent molecules occluded within the lattice which could interfere with some intermolecular interactions.

CONCLUSIONS

We have described the synthesis of four new TFXdiols: 9-trifluoromethyl-3,6-xanthenediols **I** and **II**, as well as 9-trifluoromethyl-2,7-xanthenediols **IV** and **VI**. Their molecular

https://doi.org/10.1021/acsomega.1c06635
ACS Omega 2022, 7, 13520−13528

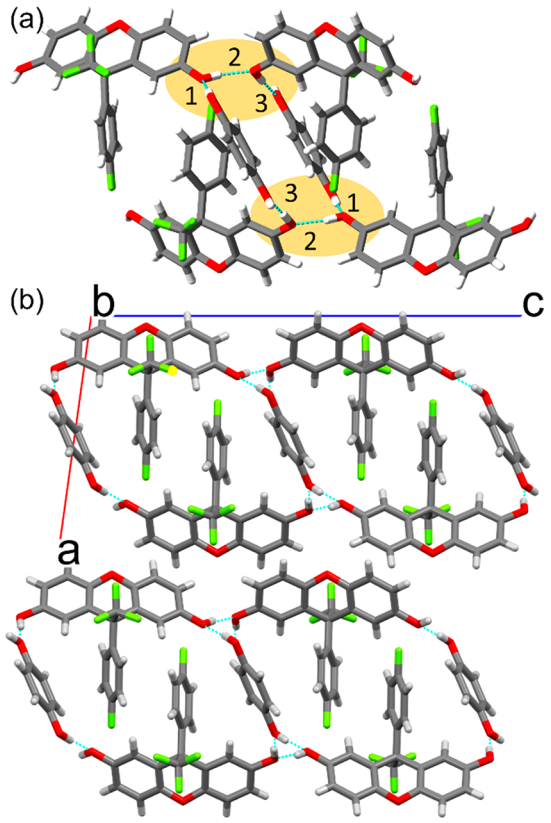

Figure 8. (a) Fourth-order ring motif of **VI** formed with hydroxyl hydrogen bonds. (b) Crystal packing of **VI** viewed through the *b*-axis.

structures were obtained through single-crystal X-ray diffraction studies and compared with the only two other examples found in the literature (molecules **III** and **V**). Despite the size and shape of the TFXdiols, their appended hydroxyl groups show conformations similar to those found in the smaller resorcinol. It was found that when the −OH groups are in positions 3 and 6, they adopt either anti−anti or anti−syn arrays to afford molecular packings where hydrogen bonds propagate across all directions. On the other hand, only syn−syn arrays are observed when the hydroxyl groups are in positions 2 and 7, giving rise to layers. Despite the differences in the relative positions of the OH groups, there is a high degree of similarity in the molecular conformations; however, the packings are considerably different. Finally, the analysis of structure **VI** indicates that the TFXdiols can be used as a platform to obtain new cocrystals in the future. We consider that the work presented here is timely because it provides the conformations and molecular packing of scarcely explored xanthenediols.

■ ASSOCIATED CONTENT

Supporting Information

The Supporting Information is available free of charge at https://pubs.acs.org/doi/10.1021/acsomega.1c06635.

X-ray refinement details and NMR solution spectra (PDF)

Crystallographic information files for **I**, **III**, **IV**, **VI** (CIF1, CIF2, CIF3, CIF4)

Accession Codes

CCDC Deposition Nos. 2122963−2122966 contain the supplementary crystallographic data for this paper. These data can be obtained free of charge via www.ccdc.cam.ac.uk/data_request/cif, or emailing data_request@ccdc.cam.ac.uk, or by contacting The Cambridge Crystallographic Data Centre, 12 Union Road, Cambridge CB2 1EZ, UK; fax: +44 1223 336033.

■ AUTHOR INFORMATION

Corresponding Authors

Manuel Rodríguez-Molina − *Instituto de Investigaciones en Materiales, Universidad Nacional Autónoma de México, 04510 Ciudad de México, México;* Present Address: PPG-Industries, Polymer Research Center, Tepexpan, Acolman, 55885, Estado de México, México; Email: jmrodriguez@ppg.com

Braulio Rodríguez-Molina − *Instituto de Química, Universidad Nacional Autónoma de México, 04510 Ciudad de México, México;* orcid.org/0000-0002-1851-9957; Email: brodriguez@iquimica.unam.mx

Authors

Dazaet Galicia-Badillo − *Instituto de Química, Universidad Nacional Autónoma de México, 04510 Ciudad de México, México;* orcid.org/0000-0002-0705-6045

Enoc Cetina-Mancilla − *Instituto de Investigaciones en Materiales, Universidad Nacional Autónoma de México, 04510 Ciudad de México, México*

Jorge Cárdenas − *Instituto de Química, Universidad Nacional Autónoma de México, 04510 Ciudad de México, México*

Lilian I. Olvera − *Instituto de Investigaciones en Materiales, Universidad Nacional Autónoma de México, 04510 Ciudad de México, México;* orcid.org/0000-0002-1505-2319

Rubén A. Toscano − *Instituto de Química, Universidad Nacional Autónoma de México, 04510 Ciudad de México, México*

Mikhail G. Zolotukhin − *Instituto de Investigaciones en Materiales, Universidad Nacional Autónoma de México, 04510 Ciudad de México, México;* orcid.org/0000-0001-7395-7354

Complete contact information is available at: https://pubs.acs.org/10.1021/acsomega.1c06635

Notes

The authors declare no competing financial interest.

■ ACKNOWLEDGMENTS

D.G.-B. thanks CONACYT for the scholarship (763328). This project was supported by CONACYT (A1-S-32820 and A1-S-17967, 251693) and PAPIIT (IN103920 and IA100321). The authors are in debt to O. J. Alvarez, E. R. Morales, and M. E. Hernandez for help with structural characterizations and to A. Lopez-Vivas and Alejandro Pompa for technical help.

■ REFERENCES

(1) Poupelin, J. P.; Saint Ruf, G.; Foussard Blanpin, O. Synthese et Proprietes Anti Inflammatoires de Derives Du Bis (Hydroxy 2 Naphtyl 1) Methane. I. Derives Monosubstitues. *Eur. J. Med. Chem.* **1978**, *13* (1).

(2) Rewcastle, G. W.; Atwell, G. J.; Zhuang, L.; Baguley, B. C.; Denny, W. A. Potential Antitumor Agents. 61. Structure-Activity Relationships for in Vivo Colon 38 Activity among Disubstituted 9-Oxo-9H-Xanthene-4-Acetic Acids. *J. Med. Chem.* **1991**, *34* (1), 217−222.

(3) Wang, H.; Lu, L.; Zhu, S.; Li, Y.; Cai, W. The Phototoxicity of Xanthene Derivatives against Escherichia Coli, Staphylococcus Aureus, and Saccharomyces Cerevisiae. *Curr. Microbiol.* **2006**, *52* (1), 1.
(4) Bhattacharya, A. K.; Rana, K. C.; Mujahid, M.; Sehar, I.; Saxena, A. K. Synthesis and in Vitro Study of 14-Aryl-14H-Dibenzo[a.j]-Xanthenes as Cytotoxic Agents. *Bioorg. Med. Chem. Lett.* **2009**, *19* (19), 5590.
(5) Hafez, H. N.; Hegab, M. I.; Ahmed-Farag, I. S.; El-Gazzar, A. B. A. A Facile Regioselective Synthesis of Novel Spiro-Thioxanthene and Spiro-Xanthene-9′,2-[1,3,4]Thiadiazole Derivatives as Potential Analgesic and Anti-Inflammatory Agents. *Bioorg. Med. Chem. Lett.* **2008**, *18* (16), 4538.
(6) Saint-Ruf, G.; Huynh-Trong-Hieu; Poupelin, J. P. The Effect of Dibenzoxanthenes on the Paralyzing Action of Zoxazolamine. *Naturwissenschaften* **1975**, *62* (12), 584.
(7) Lin, S.; Sin, W. L. W.; Koh, J. J.; Lim, F.; Wang, L.; Cao, D.; Beuerman, R. W.; Ren, L.; Liu, S. Semisynthesis and Biological Evaluation of Xanthone Amphiphilics as Selective, Highly Potent Antifungal Agents to Combat Fungal Resistance. *J. Med. Chem.* **2017**, *60* (24), 10135−10150.
(8) Sarma, R. J.; Baruah, J. B. One Step Synthesis of Dibenzoxanthenes. *Dye. Pigment.* **2005**, *64* (1), 91.
(9) Banerjee, A.; Mukherjee, A. K. Chemical Aspects of Santalin as a Histological Stain. *Biotechnol. Histochem.* **1981**, *56* (2), 83.
(10) Ahmad, M.; King, T. A.; Ko, D. K.; Cha, B. H.; Lee, J. Performance and Photostability of Xanthene and Pyrromethene Laser Dyes in Sol-Gel Phases. *J. Phys. D. Appl. Phys.* **2002**, *35* (13), 1473.
(11) Bhowmik, B. B.; Ganguly, P. Photophysics of Xanthene Dyes in Surfactant Solution. *Spectrochim. Acta - Part A Mol. Biomol. Spectrosc.* **2005**, *61* (9), 1997.
(12) El-Brashy, A. M.; El-Sayed Metwally, M.; El-Sepai, F. A. Spectrophotometric Determination of Some Fluoroquinolone Antibacterials by Binary Complex Formation with Xanthene Dyes. *Farmaco* **2004**, *59* (10), 809.
(13) Klimtchuk, E.; Rodgers, M. A. J.; Neckers, D. C. Laser Flash Photolysis Studies of Novel Xanthene Dye Derivatives. *J. Phys. Chem.* **1992**, *96* (24), 9817.
(14) Deo, C.; Abdelfattah, A. S.; Bhargava, H. K.; Berro, A. J.; Falco, N.; Farrants, H.; Moeyaert, B.; Chupanova, M.; Lavis, L. D.; Schreiter, E. R. The HaloTag as a General Scaffold for Far-Red Tunable Chemigenetic Indicators. *Nat. Chem. Biol.* **2021**, *17* (6), 718−723.
(15) Yao, F. L.; Sheng, S. R.; Jiang, J. W.; Liu, X. L.; Song, C. S. Soluble Copoly(Aryl Ether Ether Ketone Ketone)s Containing Xanthene and Hexafluoroisopropylidene Moieties. *J. Fluor. Chem.* **2012**, *144*, 176.
(16) Fernandes, J. A.; Morisaki, Y.; Chujo, Y. Aromatic Ring-Layered Polymer Containing 2,7-Linked Carbazole on Xanthene. *Polym. Bull.* **2010**, *65* (5), 465.
(17) Morisaki, Y.; Fernandes, J. A.; Chujo, Y. Xanthene-Based Oligothiophene-Layered Polymers. *Macromol. Chem. Phys.* **2010**, *211* (22), 2407.
(18) Fernandes, J. A.; Morisaki, Y.; Chujo, Y. Aromatic-Ring-Layered Polymers Composed of Fluorene and Xanthene. *Polym. J.* **2011**, *43* (8), 733−737.
(19) Chen, Q.; Luo, M.; Wang, T.; Wang, J. X.; Zhou, D.; Han, Y.; Zhang, C. S.; Yan, C. G.; Han, B. H. Porous Organic Polymers Based on Propeller-like Hexaphenylbenzene Building Units. *Macromolecules* **2011**, *44* (14), 5573.
(20) Li, X.; Zhang, Y. C.; Zhao, Y.; Zhao, H. P.; Zhang, B.; Cai, T. Xanthene Dye-Functionalized Conjugated Porous Polymers as Robust and Reusable Photocatalysts for Controlled Radical Polymerization. *Macromolecules* **2020**, *53* (5), 1550−1556.
(21) Cai, Z.; Liu, Y.; Wang, C.; Xie, W.; Jiao, Y.; Shan, L.; Gao, P.; Wang, H.; Luo, S. Ladder Polymers of Intrinsic Microporosity from Superacid-Catalyzed Friedel-Crafts Polymerization for Membrane Gas Separation. *J. Membr. Sci.* **2022**, *644*, 120115.
(22) Zuo, P.; Li, Y.; Wang, A.; Tan, R.; Liu, Y.; Liang, X.; Sheng, F.; Tang, G.; Ge, L.; Wu, L.; Song, Q.; McKeown, N. B.; Yang, Z.; Xu, T. Sulfonated Microporous Polymer Membranes with Fast and Selective Ion Transport for Electrochemical Energy Conversion and Storage. *Angew. Chem.* **2020**, *132* (24), 9651−9660.
(23) Tao, L.; Yang, H.; Liu, J.; Fan, L.; Yang, S. Synthesis and Characterization of Highly Optical Transparent and Low Dielectric Constant Fluorinated Polyimides. *Polymer (Guildf).* **2009**, *50* (25), 6009.
(24) Tao, L.; Yang, H.; Liu, J.; Fan, L.; Yang, S. Synthesis of Fluorinated Polybenzoxazoles with Low Dielectric Constants. *J. Polym. Sci. Part A Polym. Chem.* **2010**, *48* (21), 4668.
(25) Volksen, W.; Miller, R. D.; Dubois, G. Low Dielectric Constant Materials. *Chem. Rev.* **2010**, *110* (1), 56.
(26) Dhara, M. G.; Banerjee, S. Fluorinated High-Performance Polymers: Poly(Arylene Ether)s and Aromatic Polyimides Containing Trifluoromethyl Groups. *Prog. Polym. Sci.* **2010**, *35*, 1022−1077, DOI: 10.1016/j.progpolymsci.2010.04.003.
(27) Olvera, L. I.; Zolotukhin, M. G.; Hernández-Cruz, O.; Fomine, S.; Cárdenas, J.; Gaviño-Ramírez, R. L.; Ruiz-Trevino, F. A. Linear, Single-Strand Heteroaromatic Polymers from Superacid-Catalyzed Step-Growth Polymerization of Ketones with Bisphenols. *ACS Macro Lett.* **2015**, *4* (5), 492.
(28) Olvera, L. I.; Rodríguez-Molina, M.; Ruiz-Trevino, F. A.; Zolotukhin, M. G.; Fomine, S.; Cárdenas, J.; Gavino, R.; Alexandrova, L.; Toscano, R. A.; Martínez-Mercado, E. A Highly Soluble, Fully Aromatic Fluorinated 3D Nanostructured Ladder Polymer. *Macromolecules* **2017**, *50* (21), 8480−8486.
(29) Groom, C. R.; Bruno, I. J.; Lightfoot, M. P.; Ward, S. C. The Cambridge Structural Database. *Acta Crystallogr.* **2016**, *B72*, 171−179.
(30) Bruno, I. J.; Cole, J. C.; Edgington, P. R.; Kessler, M.; Macrae, C. F.; McCabe, P.; Pearson, J.; Taylor, R. New Software for Searching the Cambridge Structural Database and Visualizing Crystal Structures. *Acta Crystallogr.* **2002**, *B58*, 389−387.
(31) Chen, Y. H.; He, J. B.; Bai, X.; Li, X. N.; Lu, L. F.; Liu, Y. C.; Zhang, K. Q.; Li, S. H.; Niu, X. M. Unexpected Biosynthesis of Fluorescein-Like Arthrocolins against Resistant Strains in an Engineered Escherichia Coli. *Org. Lett.* **2019**, *21* (16), 6499−6503.
(32) Storch, G.; Kim, B.; Mercado, B. Q.; Miller, S. J. A Stereodynamic Redox-Interconversion Network of Vicinal Tertiary and Quaternary Carbon Stereocenters in Hydroquinone−Quinone Hybrid Dihydrobenzofurans. *Angew. Chemie - Int. Ed.* **2018**, *57* (46), 15107−15111.
(33) Ramon, G.; Coleman, A. W.; Nassimbeni, L. R.; Taljaard, B. Inclusion of Aromatic Guests by a Xanthenol Host: Structures, Guest Exchange, and Desorption Kinetics. *Cryst. Growth Des.* **2005**, *5* (6), 2331.
(34) Curtis, E.; Nassimbeni, L. R.; Su, H.; Taljaard, J. H. Xanthenol Clathrates: Structures and Solid-Solid Reactions. *Cryst. Growth Des.* **2006**, *6* (12), 2716.
(35) da Silva, M. L.; Teixeira, R. R.; de Oliveira, F. M.; de Moura Guimarães, L.; Martins, F. T. Vibrational Spectroscopic Studies, Theoretical Aspects, and X-Ray Analysis of Xanthenodiones (1,8-Dioxooctahydroxanthenes). *J. Heterocycl. Chem.* **2021**, *58* (3), 777.
(36) Kavala, V.; Murru, S.; Patel, B. K.; Das, G. Self-Assembled Superstructure of Xanthene Derivatives. *J. Chem. Crystallogr.* **2007**, *37* (8), 527.
(37) Bučar, D. K.; Filip, S.; Arhangelskis, M.; Lloyd, G. O.; Jones, W. Advantages of Mechanochemical Cocrystallisation in the Solid-State Chemistry of Pigments: Colour-Tuned Fluorescein Cocrystals. *CrystEngComm* **2013**, *15* (32), 6289.
(38) Tao, L.; Yang, H.; Liu, J.; Fan, L.; Yang, S. Synthesis and Characterization of Fluorinated Bisphenols and Tetraphenols via a Simple One-Pot Reaction. *Synth. Commun.* **2013**, *43* (17), 2319−2325.
(39) Safari, F.; Olejniczak, A.; Katrusiak, A. Pressure-Dependent Crystallization Preference of Resorcinol Polymorphs. *Cryst. Growth Des.* **2019**, *19* (10), 5629−5635.
(40) MacGillivray, L. R.; Reid, J. L.; Ripmeester, J. A. Supramolecular Control of Reactivity in the Solid State Using Linear

Molecular Templates [4]. *J. Am. Chem. Soc.* **2000**, *122* (32), 7817−7818.
(41) Mukherjee, A.; Grobelny, P.; Thakur, T. S.; Desiraju, G. R. Polymorphs, Pseudopolymorphs, and Co-Crystals of Orcinol: Exploring the Structural Landscape with High Throughput Crystallography. *Cryst. Growth Des.* **2011**, *11* (6), 2637−2653.
(42) Rohlíček, J.; Skořepová, E.; Babor, M.; Čejka, J. CrystalCMP: An Easy-to-Use Tool for Fast Comparison of Molecular Packing. *J. Appl. Crystallogr.* **2016**, *49* (6), 2172−2183.
(43) Steiner, T. The Hydrogen Bond in the Solid State. *Angew. Chemie Int. Ed.* **2002**, *41* (1), 48−76.
(44) Yao, Z.-F.; Wang, J.-Y.; Pei, J. Control of $\pi-\pi$ Stacking via Crystal Engineering in Organic Conjugated Small Molecule Crystals. *Cryst. Growth & Des.* **2018**, *18* (1), 7−15.
(45) Schollmeyer, D.; Shishkin, O. V.; Ruhl, T.; Vysotsky, M. O. OH − p and Halogen − p Interactions as Driving Forces in the Crystal Organisations of Tri-Bromo and Tri-Iodo Trityl Alcohols. *CrystEngComm* **2008**, *10*, 715−723.
(46) Ramamurthy, V.; Sivaguru, J. Supramolecular Photochemistry as a Potential Synthetic Tool: Photocycloaddition. *Chem. Rev.* **2016**, *116* (17), 9914−9993.
(47) Mooibroek, T. J.; Gamez, P.; Reedijk, J. Lone Pair-π Interactions: A New Supramolecular Bond? *CrystEngComm* **2008**, *10* (11), 1501−1515.

https://doi.org/10.1021/acsomega.1c06635
ACS Omega 2022, 7, 13520−13528